Intragenus competition between coccolithoviruses: an insight on how a select few can come to dominate many.

Jozef I Nissimov[1,*], Johnathan A Napier[2], Michael J Allen[1§] and Susan A Kimmance[1],

[1]Plymouth Marine Laboratory, Prospect Place, The Hoe, Plymouth, PL1 3DH, UK

[2]Department of Biological Chemistry, Rothamsted Research, Harpenden, Herts AL5 2JQ, UK

[§]Corresponding author

[*]Current Address: Institute of Marine and Coastal Sciences, Rutgers University, New Brunswick, NJ, 08901, USA

Email addresses:

JIN: jnissimov@marine.rutgers.edu

JAN: johnathan.napier@rothamsted.ac.uk

SAK: sukim@pml.ac.uk

MJA: mija@pml.ac.uk

ABSTRACT

Viruses are a major cause of coccolithophore bloom demise in both temperate and sub-temperate oceanic regions. Here we observe the competitive interactions between two coccolithovirus strains, EhV-86 and EhV-207 during the infection of the cosmopolitan marine micro-alga *Emiliania huxleyi*. EhV-207 displayed a shorter lytic cycle and increased production potential than EhV-86, and was remarkably superior under competitive conditions. The observation of such clear phenotypic differences between genetically distinct, yet similar, coccolithovirus strains by flow cytometry and quantitative real time PCR allowed links to the burgeoning genomic, transcriptomic and metabolic data currently available to be made. We speculate on the tentative identification of the genetic source of the phenotypic variation observed and the factors driving their selection (such as the functional relevance of the encoded sphingolipid biosynthesis associated genes). This work illustrates that, even within a family, not all viruses are created equally and the potential exists for relatively small genetic changes to infer disproportionately large competitive advantages for one coccolithovirus over another, ultimately leading to a few viruses dominating the many.

Keywords: coccolithoviruses, infection dynamics, competition, phenotypes, E. huxleyi

INTRODUCTION

Viruses are a major cause of coccolithophore bloom demise in both temperate and sub-temperate oceanic regions (Bratbak et al., 1995; Martinez et al., 2007; Brussaard et al., 2008; Sorensen et al., 2009). Their role in regulating coccolithophore populations has been firmly established via studies of natural environmental systems (Wilson et al. 2002, Schroeder et al. 2003, Martinez et al. 2007), and induced semi-natural blooms in the Norwegian fjords (Bratbak et al. 1993, Jacquet et al. 2002, , Pagarete et al. 2009, , Kimmance et al. 2014). In addition to the direct reduction in total cell abundance, the species-specific nature of viruses leads to the regulation of interspecies competition and succession within a mixed phytoplankton community (Brussaard, 2004; Fuhrman, 1999).

Within a coccolithophore bloom, the success of specific coccolithovirus strains vary and is influenced, among other factors, by the type of host strains present and the physico-chemical environment in which they are found (Wilson et al., 2002a; Martinez et al., 2007, 2012; Rowe et al., 2011; Coolen, 2011). Under bloom conditions, there is typically an initial and diverse pool of low abundance virus (Sorensen et al. 2009) and host strains (Schroeder et al. 2003), a subset of which become more dominant than others as the bloom progresses (Martinez et al. 2007; Sorensen et al. 2009), and an indication that some virus genotypes win over others (Pagarete et al, 2014, Highfield et al, 2014). Virus abundance and diversity is controlled by external (environmental) influences that drive evolutionary processes (Coolen et al. 2011; Martinez et al. 2012). However, the molecular diversity observed within samples is a mere snapshot of that particular time, and although useful, it does not reveal how and why coccolithovirus strains vary with regards to infection strategies and mechanisms. Given that there are clear genetic differences between coccolithovirus isolates (Allen et al. 2006, Nissimov et al. 2011, 2012, 2014, Pagarete et al. 2013) it is likely that within a mixed

community of coccolithoviruses during bloom conditions, subtle variations in their phenotypic properties, i.e. infection and lysis rates, may have a profound impact on shaping the ultimate genetic richness and composition of the host and viral community.

However, the fundamental question remains as to how differences in coccolithovirus phenotypes influence host growth dynamics, virus succession and population survival. A previous study by Bidle and Kwityn (2012) demonstrated that different *Emiliania huxleyi* strains vary in their susceptibility to infection by a single coccolithovirus strain, yet, to date, the significance of coccolithovirus strain-specific differences have not yet been fully investigated. Whether the enormous genetic potential contained within their large genomes (~400-500 MBs) produces variations in the infection strategies employed by different coccolithovirus strains, remains to be determined. Like in all other virus systems, intra-familial competition among coccolithoviruses for successful infection and replication must exist. The molecular encoded components at the interface of this ongoing evolutionary struggle are currently unknown, yet our current whole genomic knowledge of a dozen coccolithovirus strains suggests their identification is now possible.

Here we use an experimental approach to assess the phenotypic differences in two *E. huxleyi* virus (EhV) strains, and their manifestation during infection of a single host strain. Infection experiments were performed with two coccolithovirus strains which were originally isolated from the same location in the English Channel: EhV-86 and EhV-207, and have been shown previously to successfully infect the same host (*E. huxleyi* CCMP 2090) (Nissimov et al, 2011; 2012), yet differ in genomic composition (Nissimov et al. 2014). For simplicity, it was decided that the focus would be to identify any potential differences in viral production and host lysis during infection, and not to consider host strain variability here. The main goal was

to reveal the competitive interactions of two genetically distinct viruses infecting side by side, and assess the implications for host growth and virus productivity. Strain specific primers were designed for each coccolithovirus, and the change in EhV abundance was monitored for one week post- virus addition by means of quantitative real time PCR (qPCR) and Analytical Flow Cytometry (AFC).

MATERIALS AND METHODS

Culture conditions and experimental setup

Prior to the start of the experiment, cultures of *E. huxleyi* CCMP 2090 were grown in filtered (30 kDa, TFF GE Healthcare), autoclaved natural seawater enriched with f/2 nutrients (Guillard 1975), in 2 L InforsMinifors chemostat bioreactors (INFORS UK Ltd). Cultures were maintained with a light and dark cycle of 16:8 hours, at a white light intensity of ~86 µM photons m^{-2} s^{-1}, and a temperature of 18°C, with continuous gentle mixing and aeration. *Emiliania huxleyi* abundance was measured daily using analytical flow cytometry (AFC, see below for protocol), and when cellular density reached 1.5×10^6 cells mL^{-1} (i.e. beginning of exponential growth, $\mu = > 0.7$), aliquots of 100 mL were distributed into 12 polystyrene, sterile, 250 mL tissue culture flasks (Greiner, CellStar). The 12 algal subculture flasks and nine additional flasks containing only f/2 media (controls; Table S1) were then returned to the same light and temperature conditions as above, and left to acclimatise for 48 h.

The virus pathogens EhV strain EhV86 (Wilson et al. 2002) and EhV-207 (Nissimov et al. 2012) were obtained from the Plymouth Marine Laboratory virus collection and for each EhV strain, a fresh batch of viral lysate was prepared prior to experiments to ensure a high amount of infective virions. For this, 500 mL of an exponentially growing *E. huxleyi* CCMP2090 culture (~4×10^6 cells mL^{-1}) was infected with 5-10 mL of an EhV lysate stock. When the

culture had lysed (complete loss of pigmentation, monitored using analytical flow cytometry, AFC, see below) lysates were gently vacuum-filtered through 0.2 µm pore size sterile filters, Millipore Express) to remove *E. huxleyi* cell debris, and stored in the dark at 4°C until required. On the day of the experiment (t0), the experimental flasks were set up to represent seven different treatments (A-G) as described in Table S1. Ten minutes before the first sampling point (t0), flasks 1-3 (A) were inoculated with EhV-86 lysate at a virus:host ratio of 1:1; flasks 4-6 (B) were inoculated with EhV-207 at a virus:host ratio of 1:1; and flasks 7-9 (C) were inoculated with a combination of both EhV-86 and EhV-207, providing an overall virus:host ratio of 1:1 (with a 1:1 ratio of each virus). Flasks 10-12 (D) were virus controls that contained no host (only culture media), but were inoculated with the same volume of EhV-86 lysate as flasks 1-3. Likewise, flasks 13-15 (E) contained only culture media and an inoculum of the same volume of EhV-207 lysate as flasks 4-6. Flasks 16-18 (F) contained only culture media and an inoculum of combined EhV-86 and EhV-207 lysates equivalent to that in flasks 7-9. Finally, flasks 19-21 (G) were the negative controls containing host culture with an addition of EhV-86 and EhV-207 lysates equivalent to treatments (C) and (F), however prior to addition lysates were inactivated through a series of treatments: autoclaving at 126°C, filter sterilization through 0.2 µm sterile cellulose acetate syringe filter (Gilson), followed by overnight exposure to UV light in a PCR station (Labcaire), prior to their addition to the control flasks.

Sampling procedure

Once experimental conditions were set up in the flasks the cultures were left for ten minutes to allow viruses to establish initial attachments/infections with the host cells. Then 3 mL of sample were taken out from each flask at the following time intervals: 0 (t0), 1 h (t1), 2 h (t2), 3 h (t3), 4 h (t4), 8 h (t5), 12 h (t6), 24 h (t7), 48 h (t8), 72 h (t9), 96 h (t10), 120 h (t11), 144

h (t12), and 168 h (t13). The 3 mL samples were then further divided into three sub-samples: 1 mL was fixed with 0.5% (final conc.) glutaraldehyde for the enumeration of host abundance using analytical flow cytometry (AFC), and 1 mL was centrifuged at 20,000g for 30 sec., of which the top phase was carefully removed into a sterile, 2 mL Eppendorf polypropylene tube, fixed with 0.5% (final conc.) glutaraldehyde, and the pellet re-suspended in 1 mL of DNA free water and fixed in 0.5 % glutaraldehyde for the subsequent enumeration of free and attached VLPs respectively by AFC. All samples were snap frozen in liquid nitrogen (LN_2) and stored at -80°C for further analysis. The same procedure was performed with the third 1 mL subsample, with the exception of the addition of the glutaraldehyde, as these samples were used for DNA extractions and subsequent quantitative real time PCR analysis.

Enumeration of host and virus abundance

All samples were analysed *en masse* following the conclusion of the experiment. Fixed, frozen samples were defrosted at room temperature and then analysed using AFC following standard protocols (Marie et al. 2000; Brussaard et al. 2004). Samples were analysed on a FACScan flow cytometer (Becton Dickinson, Oxford, UK) equipped with a 15 mW laser exciting at 488 nm and with a standard filter set up. Counts of *E. huxleyi* were conducted at high flow rate (~ 80 μL min^{-1}) and files were analysed using WinMDI 2.8 software (Joseph Trotter, [http://facs.scripps.edu]. For virus analysis, sub-samples were diluted 500-fold with TE buffer (10 mmol L^{-1} Tris-HCL pH8, 1 mmol L^{-1} EDTA), stained with SYBR Green 1 (Molecular Probes; Marie et al., 2000) at a final dilution of 5×10^{-5} the commercial stock, incubated at 80°C for 10 min in the dark, then allowed to cool for 5 min before flow cytometric analysis. Samples were analysed at a flow rate of ~ 20 μL min^{-1} and EhVs were identified on the basis of their RALS versus green fluorescence. Data files were analysed using WinMDI 2.8 software (as above). The two EhV strains could not be separated by their

AFC profiles in the combined EhV-86 and EhV-207 treatments, as they gave identical fluorescence vs. scatter signatures.

Probe design and optimisation

The selection for specific primer probes for the two viruses EhV-86 and EhV-207 was performed on the IMG/ER analysis platform, in which the total protein coding genes of EhV-86 and EhV-207 were BLAST searched against each other with a maximum E value of $1e^{-05}$ and minimum percent identity of 40%. Following this analysis, EhV-86 and EhV-207 strain specific genes were identified (i.e. ehv290 [510 bp] and EQVG00465 [1059 bp], respectively) and selected for the design of strain specific PCR primers. The final sequence lengths that were to be amplified by PCR/quantitative real time PCR were 209 bp and 353 bp for EhV-86 and EhV-207 respectively (primers sequence: qPCR(EhV-86)-F [5'-GCACAACTTTCAACAATTCG-3']; qPCR(EhV-86)-R [5'-TCAGCTCAACTTTTGGATCA-3']; qPCR(EhV-207)-F [5'CATAGGGTTGGCAATATTCA-3'] and qPCR(EhV-207)-R [5'-TTCGAAACAACTTGGTCAAC-3'], Sigma-Aldrich Company Ltd).

To first establish that the designed primers were strain specific, a standard PCR was performed on fresh lysate stocks of EhV-86 and EhV-207 with the primers for ehv290 (i.e. qPCR(EhV-86)-F and qPCR(EhV-86)-R) and EQVG00465 (i.e. qPCR(EhV-207)-F) and qPCR(EhV-207)-R). Reactions were conducted in a VWR JENCONS Uno Thermal Cycler in 25 µL final volume reactions (unless otherwise stated). PCR reactions were set as follows: 1 µL of virus lysate template (or ~50 ng μL^{-1} of extracted DNA) was mixed with 5 µL of 1 × PCR reaction buffer (Promega), 1.5 µL of 25 mM $MgCl_2$, 0.1 µL of *Taq* DNA polymerase (Promega), 2 µL of 10 µM of each primer, 1.25 µL of 2 mM dNTPs and DNA-free molecular biology grade water (Sigma-Aldrich). PCR was conducted in triplicate and the conditions

were as follows: an initial denaturation step at 95°C for 3 min, followed by 34 cycles at 95°C, 60°C and 74°C for 30, 60 and 90 sec respectively, and a final cycle at 95°C, 60°C and 74°C for 30 sec, 5 min and 5 min respectively.

DNA extraction from top phase and pellet samples

Phenol-chloroform DNA extraction was performed on the samples intended for qPCR analysis based on the detailed protocol described by Schroeder et al, (2002). Briefly, 0.5 mL aliquots from the 1 mL top phase and pelleted sub-samples collected at the different time points during the experiment were placed into sterile tubes in a heating block at 90°C for 1 min and then transferred onto ice for a further minute, repeating this three times. Then to the tubes were added 20 µL 0.5 M EDTA pH 8.0 at a final concentration of 20 mM, 5 µL proteinase K at a final concentration of 50 µg mL^{-1}, and 25 µL of 10% SDS at a final concentration of 0.5%, and incubated in a water bath for 1 h at 65°C. After the incubation the tubes were transferred onto ice and gently mixed with 60 µL of phenol. Then 500 µL of chloroform/isoamyl alcohol (24:1) was added to the tubes, mixed gently, after which they were centrifuged at 10,000 rpm for 5 min. After removing the top phase into a clean Eppendorf microfuge tube and adding 500 µL of 7.5 M ammonium acetate, they were left at room temperature for 30 min. A centrifugation step at 10,000 rpm for 15 min followed after which the supernatants were placed into clean 2 mL Eppendorf tubes. To these tubes 1 mL of 100% ethanol (ETOH) was added, leaving them to precipitate for 3 h at 4°C, and then centrifuging them at 13,000 rpm for 30 min after which the supernatants were removed and discarded. Finally, the pellets were washed by centrifugation for 10 min with 500 µL of 70% ETOH and air dried overnight. The genomic DNA pellets were re-suspended in 50 µL of TE buffer and then quantified by spectrophotometer (i.e. NanoDrop) and a 1% agarose gel electrophoresis.

Quantitative real-time PCR

Quantitative real-time PCR (qPCR) assays on extracted DNA samples were carried out in optical-grade 96-well plates in an ABI PRISM®7000 Sequence Detection System (Applied Biosystems, UK) with the Qiagen Quantifast Sybr Green PCR kit containing a ready to use master mix. The calibration curve (or standards) for the qPCR to which each experiment DNA sample was compared to consisted of triplicates of the serial dilutions (10^{-1} to 10^{-10}) of amplified and gel extracted PCR products of ehv290 (for EhV-86) and EQVG00465 (for EhV-207) at initial DNA concentrations of 65.7 ng μL^{-1} and 57.4 ng μL^{-1} respectively (i.e. predicted DNA copy number of 2.91×10^{11} and 1.51×10^{11} μL^{-1} respectively). The calibration curve diluted samples were loaded each time on the same plate as the DNA samples from the experiment in order to reduce bias occurring due to small shifts in fluorescence signal from one 96 well plate to another. The reactions of both standards and samples consisted of 12.5 µL of Sybr Green master mix, 0.5 µL of primer qPCR(EhV-86)-F or qPCR(EhV-207)-F (at a final conc. of 0.2 µM), 0.5 µL of primer qPCR(EhV-86)-R or qPCR(EhV-207)-R (at a final conc. of 0.2 µM), 1 µL of template DNA (sample, standard, or NTC [no template control]) and 10.5 µL of RNAse free water (final volume of 25 µL). The thermal cycling conditions (on the ABI PRISM 7000 cycler) were as follows: an initial cycle of 95ºC for 10 min followed by 40 cycles at 95ºC for 30 sec and 60ºC for 30 sec. The automated generation of the calibration curve by the ABI PRISM 7000 sequence detection system allowed the logarithmic plotting of each standard concentration against the cycle number at which the detected fluorescence signal increased above the threshold value- CT. Then, the Sequence Detection System software calculated the target gene DNA copy number (or concentration) from the CT value obtained for each of the samples with unknown concentration. The calibration curve slope was used to determine the reaction efficiency (E) using the following equation: $E= -1+10^{(-1/slope)}$. For instance, if E equalled to 1 then this meant a 100% product doubling in each amplification cycle.

Oligonucleotide specificity

PCR amplification of EhV-86, EhV-207 and EhV-86+EhV-207-combined lysates revealed that the newly designed qPCR primers were strain specific (Fig. S1). When each set of primers was used in a sample from which the target strain was not present (EhV-86 or EhV-207), amplification was not detected; i.e. the amplification was specific to the set of primers used and only samples that had the target strain produced PCR amplicons. The amplified products of the EhV-86 and EhV-207 specific targets corresponded to the predicted size fragments of 209 and 353 bp for EhV-86 and EhV-207 respectively.

Calibration curve efficiencies of the quantitative real time PCR sample analysis

The calibration curves (Fig. S2) that were conducted to establish the optimum conditions for the qPCR analysis indicated that under the described PCR conditions, the serial dilutions of the known concentrations of ehv290 (for EhV-86) and EQVG00465 (for EhV-207) PCR generated DNA was log-linear for both, with a correlation coefficient (R^2) of 0.99. The calculated efficiency ($E= -1+10^{(-1/slope)}$) of the reactions were 102.21 % and 88.70 % respectively. The calibration curves were interrogated to allow the accurate quantification of DNA template in both single and dual infection samples.

RESULTS

Genetically distinct viruses produce contrasting host lysis rates

Emiliania huxleyi CCMP 2090 abundance increased steadily in all flasks during the first 24 h to an average (±SD) maximum of $2.6 \times 10^6 \pm 4 \times 10^5$cells mL^{-1} (Fig. 1). However, by day 3, both the EhV-207 and EhV-86+EhV-207-infected populations crashed dramatically, with a

96 % loss of cells in these flasks from $2.48 \times 10^6 \pm 2.73 \times 10^5$ (SD) to $9.83 \times 10^4 \pm 2.87 \times 10^4$ cells mL^{-1} (SD). The crash was simultaneous between these two treatments (Fig. 1). In contrast, during the same time period (24-72 h post-addition of virus), there was a 14% increase in *E. huxleyi* abundance in the EhV-86 infected cultures to 3.15×10^6 cells mL^{-1} $\pm 1.41 \times 10^5$ (SD). However by 96 h host density also began to decrease in the EhV-86 infected cultures, but at a much slower rate (~17 % reduction in host cell density) compared to the EhV-207 and EhV-86+EhV-207-infected cultures (Fig.1). These differences were also evident from the fluorescence profiles of *E. huxleyi* derived during the AFC analysis (Fig. 2) in which the mean cellular red fluorescence (proxy for chlorophyll *a*) at 72 h post-infection, was much lower in the EhV-207 and EhV-86+EhV-207-infected cultures than in those infected only with EhV-86. By the end of the experiment (168 h), the majority of the *E. huxleyi* cells in the EhV-86 infected cultures had lysed (Figs.1, 2). However a small, relatively healthy (as indicated by high cellular red fluorescence observed during AFC analysis) host population remained in the EhV-86 infected cultures, and the average (±SD) cell abundance was 2.77×10^5 ($\pm 6.89 \times 10^4$ mL^{-1}), as opposed to 2.52×10^2 ($\pm 3.36 \times 10^1$ mL^{-1}) and 1.18×10^3 ($\pm 1.24 \times 10^3$ mL^{-1}) in the EhV-207 and EhV-86+EhV-207-infected cultures respectively. With regards to the control cultures that contained inactivated EhVs, *E. huxleyi* abundance remained high at the end of the experiment with 4.32×10^6 cells mL^{-1} $\pm 3.04 \times 10^5$ (SD), (Fig. 1, 2).

EhV abundance decreased in all non-control flasks two hours post-infection to an average (±SD) of $2.91 \times 10^5 \pm 1.42 \times 10^4$ mL^{-1} (Fig. 3). This suggests that by two hours post-virus addition, almost half (45%) of the inoculated EhVs were either attached to the host cell receptors or had penetrated into the cells for replication. The first round of mass EhV release from the infected cells in all treatments was 3 h post-addition (Fig. 3). After this point there

appeared to be a separation between EhV treatments, with the samples containing EhV-207 producing a higher number of virions compared to those containing EhV-86. However, this was not statistically significant until (8 h post-addition) when there was significantly more free EhVs in the EhV-207 and EhV-86+EhV-207 infected cultures than in the EhV-86 infected treatments ($P<0.05$). The trend of significantly lower and slower virion production/release from the EhV-86 infected cultures continued until the end of the experiment 7 days post-addition ($P<0.01$). At this point, the amount of free EhV mL^{-1} in the EhV-86 infected cultures ($5.19 \times 10^7 \pm 3.88 \times 10^6$ SD) was on average 92% less than in the EhV-207-infected ($6.58 \times 10^8 \pm 1.09 \times 10^8$ SD) or EhV-86+EhV-207 ($7.04 \times 10^8 \pm 8.55 \times 10^7$ SD) combined treatments (Fig. 3). Throughout the experiment, there was no difference in the number of EhV between cultures infected by EhV-207 and those infected with both EhV-86+EhV-207 combined, with the exception of one hour post-infection, where the number of free EhVs in the combined virus treatment was significantly lower ($P<0.05$) (Fig. 3).

Quantifying strain-specific differences in virus genome copy number

Quantitative real time PCR analysis (qPCR) was used to determine EhV-86 and EhV-207 genome copy number (GCN) in both cell-free and cell-associated fractions. Total GCN estimates were derived from a combination of the two fractions. Cell-associated GCN will include genomes found within virions adsorbed to the cell surface, unreleased intracellular virions, as well as unpackaged genomes undergoing replication. Cell-free GCN estimates, on the assumption that one virus genome copy is found per free floating virion, can be directly compared to the AFC measurements of non-cell associated virions. This comparison, of EhV virion abundance determined by AFC with genome copy number quantified by qPCR, revealed that there was a consistent 100-fold decrease in the predicted genome copy number detected by the qPCR method, a phenomena most likely caused due to inefficiencies during

312 the phenol-chloroform DNA extraction step (Table S2). This reduction in apparent virus
313 abundance was consistent throughout the experiment and was thus taken into consideration
314 when interpreting the qPCR results of the dual virus infection treatments. In addition, the
315 resolution of the qPCR was accurate only 12 h post-EhV addition at GCN higher than 10^3
316 mL^{-1}, hence the qPCR results of t0 – t5 were below reliable detection levels and are not
317 shown here. Regardless of whether the two virus strains were added to the host cultures
318 combined or in isolation, EhV-207 and EhV-86 appeared to exhibit different infection
319 dynamics, and the qPCR results revealed more than what was initially observed with the AFC
320 analysis alone.
321
322 In the single virus-addition treatments, EhV-207 exhibited faster infection than EhV-86 and
323 replicated to produce new virions quicker; i.e. combined GCN was higher (Fig. 4). In the dual
324 infection treatments (EhV-207 + EhV-86), the presence of EhV-86 did not appear to reduce
325 the infection potential of EhV-207, and GCN produced was comparable to that in the EhV-
326 207-only infected treatments. In contrast, EhV-86 was affected by the presence of EhV-207
327 in the dual infection treatments and the amount of EhV-86 GCN at the end of the experiment
328 was 1000 fold less than in the single EhV-86 infected cultures ; i.e. $6 \times 10^3 \pm 2.86 \times 10^3$ (SD)
329 and $4 \times 10^6 \pm 1.28 \times 10^6$ (SD) mL^{-1} respectively (Fig. 4). Thus, EhV-207 appeared to be not
330 only a faster strain than EhV-86 with regards to its rate of infection under the conditions
331 studied, but also a 'superior' strain that out-competed its EhV-86 rival to infect a host
332 population when they were combined at equal abundance
333
334 To gain a deeper understanding of the competitive interactions between the two EhVs, we
335 also measured the GCN of each virus strain that was associated with the cellular fraction,
336 with the assumption that the GCN in the pelleted fraction represents viruses or synthesised

337 viral genomes within the cells or virus particles attached to the cell receptors (infecting or
338 still attached). Throughout the experiment, the amount of cell-associated EhV-207 GCN in
339 both dual and single virus treatments was higher than the amount of free EhV-207 GCN, with
340 the exception of 168 h post-infection. At this point the average (±SD) amount of free and
341 cell-associated EhV-207 GCN was equivalent: i.e. 6.9×10^6 ($\pm 2.6 \times 10^5$) and 5.59×10^6
342 ($\pm 1.01 \times 10^6$) respectively (Fig. 4). In comparison, the amount of cell-associated EhV-86
343 GCN in both dual and single virus treatments was also higher than the amount of free EhV-86
344 GCN throughout the experiment, with the exception of 12 h post infection, where the average
345 (±SD) amount of free and attached cell-associated EhV-86 GCN was equivalent: i.e. $1.27 \times$
346 10^3 ($\pm 1.85 \times 10^2$) and 1.69×10^3 ($\pm 8.6 \times 10^2$) respectively (Fig. 4).
347
348 The presence of EhV-86 in the dual infection treatments did not affect the amount of cell-
349 associated or free EhV-207, as the GCN of both fractions was similar to the GCN of the cell-
350 associated and free EhV-207 in the EhV-207 single virus treatments. At 48 h post-infection
351 the average (±SD) cell-associated EhV-207 GCNs in the dual and single virus treatments
352 were 5×10^7 ($\pm 2.83 \times 10^7$) and 4.47×10^7 ($\pm 1.52 \times 10^7$) respectively, while the average
353 (±SD) free EhV-207 GCNs in both the dual and single virus treatments were 3.89×10^6
354 ($\pm 2.62 \times 10^5$) and 5.25×10^6 ($\pm 7.07 \times 10^4$) respectively. In contrast, in the dual-infected
355 treatments the presence of EhV-207 decreased the GCN of both cell-associated and free EhV-
356 86. At 12 and 48 h post-virus addition there were 72 % and 65 % less cell-associated EhV-86
357 genomes, and 18 % and 42 % less free EhV-86 genomes in the dual infected treatments,
358 respectively, in comparison with the single virus treatments (Fig. 4).
359
360 By the end of the sampling period the cell-associated EhV-86 copy number in the dual
361 infection treatments was more than three orders of magnitude lower than that of cell-

associated EhV-207. Similarly, the average GCNs of free EhV-86 in both the single and dual infected treatments were approximately 15 and 2500 times lower respectively, than the average GCN of free EhV-207 after 168 h (Fig. 4).

DISCUSSION

To date, potential differences in infection rates between coccolithovirus strains have been assessed briefly in only one previous study (Nissimov et al, 2013), and to our knowledge this is the first time where these dynamics have been investigated under controlled laboratory conditions that includes an in-depth quantitative coccolithovirus genome analysis. Strain-specific genetic markers enabled us to differentiate production rates of two EhV strains during dual-strain *E. huxleyi* infection experiments. Assessment of the competitive interactions of these viruses during infection of the host identified major differences in their infection strategies. When infecting in combination, EhV-207 was not affected by the presence of EhV-86 whereas EhV-86 was quickly out-competed, and a significant reduction in free and cell-associated EhV-86 was seen two days after the initial infection. Thus, when infecting alongside EhV-207, the EhV-86 strain appeared to be "inferior" and its persistence in this experimental setup was under threat. The significance of the results here are fundamental in our understanding of how viruses interact with their hosts and with each other. They provide an insight into the complex and competitive interactions between viruses in the natural environment, interactions that we currently have a limited knowledge of.

The losers and winners of the virus "fight club" – a numbers game

Throughout the experiment EhV-207 appeared to be superior to EhV-86 (and perhaps more potent) in that it was a faster replicating virus with regards to its rate of infection and lysis of *E. huxleyi* CCMP 2090, regardless of the competition with EhV-86. As both virus strains

were fresh lysates produced immediately prior to the experiment, and both AFC and qPCR analysis revealed no obvious differences between the physical properties of the two strains, this suggests that they were of equivalent abundance and provenance. An equivalent number of EhVs were added at the start of the experiment (in both single and dual-virus treatments) and by 2 h post-inoculation EhV abundance in all EhV treatments decreased to an identical amount, suggesting that at least initially, there was no advantage for EhV-207 with regards to adsorption kinetics. However, by 8 h there was significantly more EhV-207 than EhV-86; suggesting that EhV-207 was able to develop a fairly rapid competitive advantage following adsorption. The dramatic increase in EhV-207 24 h post-infection in both the single and dual-virus treatments and the rapid decrease in *E. huxleyi* thereafter, demonstrates that the initial advantage following adsorption was not abated with time. If we consider this in the context of the combined-virus treatments, by generating a significant advantage over EhV-86 as early as 8 h post-infection, EhV-207 was most likely responsible for the demise of the majority of the host cells, subsequently leaving EhV-86 less hosts for its own propagation.

The mechanisms that allow EhV-207 to outcompete EhV-86 under these experimental conditions are currently not known and a future study combining a complete transcriptomic or microarray analysis during infection should be considered. Nevertheless, these results suggest that EhV-207 may have a shorter latent period within the host cells than EhV-86, and that under these experimental conditions, EhV-207 packages, assembles and releases new virus progeny much quicker than its EhV-86 rival. A second possible explanation to the EhV-207 dominance is that the amount of EhVs produced per infected host cell (burst size) was much higher when hosts were infected by EhV-207 compared to EhV-86. Over multiple rounds of reinfection, this would quickly result in EhV-207 dominating EhV-86. However, only the second explanation explains the decreased productivity of EhV-86 in comparison

412 with EhV-207 in the single virus infection treatments. Indeed, if the former were true,
413 presumably with a longer reinfection cycle, EhV-86 would be expected to produce more, not
414 less, progeny since the host cells would have longer to grow and therefore have a greater
415 overall virus production potential. Lytic viruses typically exhibit a short latent period and a
416 low burst size (Parada et al. 2006), however an extension of the latent period is a strategy
417 employed by some temperate phage during periods of low multiplicity of infection and low
418 host abundance (Wilson and Mann 1997, Parada et al. 2006). Although not measured directly
419 here, we calculated the potential burst sizes of the two EhV strains (estimated as the ratio of
420 the maximal number of viruses produced to the maximum cell concentration reached by the
421 specific host before cell decrease (Jaquet et al. 2002), as 16.5 for EhV-86 and 248 for EhV-
422 207; thus, there was potentially over an order of magnitude difference in burst size between
423 the two virus strains. Although limited, these calculations suggest that differences in burst
424 size could be a critical factor in deciding the outcome of competition dynamics between virus
425 strains.
426
427 What strategies lytic viruses such as EhVs can utilise during periods of intense competition is
428 as yet unknown, but it is clear that EhV-207 confers a competitive advantage over EhV-86
429 (ultimately affecting burst size and/or lysis rates), and the cause of such an advantage will be
430 encoded upon their respective genomes. With regards to this, EhV-207 has an extra tRNA not
431 found in the genome of EhV-86 and also 49 genes (of which 47 have no assigned or predicted
432 function) that have no homologs with EhV-86. Among these are two genes predicted to
433 encode for glycosyl-transferases (data not shown). Although rare in viruses, glycosyl-
434 transferase encoding genes have been previously reported in bacteriophages, poxviruses,
435 herpesviruses and baculoviruses (Markine-Goriaynoff et al., 2004). In some bacteriophages,
436 glycosyl-transferases have the ability to modify the virus DNA in order to protect it from host

restriction endonucleases, and in *Chlorella* viruses such as PBCV-1 they have been implicated in the synthesis of glycan components of the virus major capsid protein (Zhang et al., 2007). Hence the presence of these genes could be beneficial to EhV-207 and aid in its much increased rate of genomic assembly and capsid construction prior to release from the infected cells. It is unlikely that the genetic features unique to EhV-86 that EhV-207 does not contain (i.e. genes predicted to encode for a longevity-assurance (LAG1) family protein, a PDZ domain protein, a putative DNA-binding protein, a putative helicase, and 55 extra membrane proteins or proteins with an unknown function) act to inhibit the infection rate of EhV-86 (data not shown), although this cannot be ruled out at this stage. Alternatively, it is possible that the phenotypic difference observed is caused by functional variation in shared genetic components.

Indeed, previous studies have reported that coccolithoviruses biochemically highjack the host sphingolipid biosynthesis pathway (Pagarete et al, 2009; Bidle and Vardi, 2011; Michaelson et al, 2010) and produce virally-encoded glycosphingolipids that in turn trigger ROS (reactive oxygen species), caspase activity and PCD (programmed cell death) in the infected host cells (Bidle et al, 2007; Vardi et al, 2009, 2012). The rate limiting step in this *de novo* sphingolipid biosynthesis pathway is the first step in the reaction where serine palmitoyltransferase cleaves palmitoyl Co-A or myristoyl Co-A with serine (Han et al, 2006; Monier et al, 2009). Recent protein structural analysis has suggested that there is a difference in the protein fold of the SPT enzyme encoded by different coccolithoviruses, that may affect the rate and efficiency of this first step in the virally-encoded sphingolipid biosynthesis pathway (Nissimov et al, 2013). These potential differences between coccolithovirus strains in viral SPT activity in the first few hours post-infection may prove to be crucial in determining which strain dominates during competitive interactions such as those shown in this study.

Another facet that is worthy of consideration is the possibility that a single host cell was simultaneously infected by both virus strains. In this case, an internal intra-cellular battle over the host cellular metabolic machinery would have occurred between the two viruses. Such a scenario although theoretically possible, is maybe less likely due to the mutual exclusion theory proposed by Luria and Delbruck (1943) in which was suggested that a virus particle that infects first a host cell alters it to the extent of which a second infection by another virus is unlikely. This was indeed shown to be the case in the co-infection of *Chlorella* by two closely related viruses PBCV-1 and NY-2A (Greiner et al., 2009). In this previous study, infection by the PBCV-1 virus depolarised the host cell membrane to exclude further infections by NY-2A. Genomic comparison among EhV strains (Allen et al, 2006, Nissimov et al, 2011a, 2011b, 2012a, 2012b, 2014, and Pagarete et al, 2013) suggests that many genes have indeed been transferred between closely related virus strains, possibly a result of co-infection and retrovirus involvement (Nissimov J., PhD thesis; 2013). Hence it is not currently known whether mutual exclusion mechanisms such as the ones observed in *Chlorella* exist in coccolithoviruses, but it is worth considering and investigating further. Regardless of the mechanisms involved, EhV-86 appeared to be a poor competitor to EhV-207 and lost the battle over infection and replication when placed into direct competition with its intragenus opponent.

Finally, investigating the differences in free EhV GCN compared to the cell-associated EhV GCN revealed an aspect never previously observed in the study of coccolithovirus replication. For both EhV strains, cell-associated GCN was higher than the free GCN, suggestive that not all the newly synthesized genomes were able to be packed into virions and released from the cells. This is indicative of a nucleotide independent factor that limits the

burst size of these two EhV strains and ultimately the amount of new virus progeny produced. The EhV virion consists of dsDNA genomic material encased within a protein shell (predominantly composed of the major capsid protein), enveloped by a lipid membrane. GCN clearly indicates the production of genomic material is not limiting, therefore either protein production or membrane lipid availability and integrity are the likely limiting factors. The latter is of particular interest considering the acquisition of the near complete pathway for the synthesis of sphingolipids from the host by the coccolithoviruses, and the prominent role of such lipids in the formation of membrane rafts to instigate virus release.

The ecological significance of the virus "fight club"

To date, virus-induced decline of algal populations in the natural environment are often viewed as a one dimensional battle between hosts and their viruses. However the additional element of competition between viruses is fundamental when trying to predict viral-induced impacts on primary productivity and the role of viruses as ecological drivers of diversity. Although a laboratory study, the results here may also be representative of natural systems, where indeed there is mounting evidence that such processes occur. For instance, natural coccolithophore assemblages in the North Sea, Norwegian fjords, English coast, and the vast Atlantic Ocean, were characterised by extremely numerous and diverse co-occurring coccolithovirus communities (Wilson et al., 2002; Martinez et al., 2007, 2012, Rowe et al, 2011, Nissimov et al, 2013). In a recent mesocosm experiment in the Norwegian fjord (Sorensen et al., 2009), it was observed that the number of distinct EhV genotypes decreased with the propagation of an *E. huxleyi* infection; i.e. early on during the development of the bloom the EhV community was more diverse, and there were more distinct EhV genotypes (detected by DGGE) than towards the end of the bloom (Martinez et al, 2007, 2012; Sorensen et al, 2009). Hence the dominance of certain coccolithovirus strains over others will be a

direct consequence of competitive interactions and the specific phenotypic characteristics manifested during host-virus infection dynamics. Depending on the virus strain type/s present in a particular environment and its/their succession over other virus strains, such variation in phenotypic characteristics will affect the overall propagation of an infection, its outcome with regards to the demise of the host population, and subsequently the rates of carbon and nutrient recycling (Wilhelm and Suttle, 1999). Thus if we exclude other factors such as grazing and nutrient limitation from the equation, the ecological significance under the described scenario (i.e. EhV-207-like viruses dominating) would be a localised short-time rapid increase in the rate of carbon export and recycling of nutrients, but a reduced overall carbon and nutrient export, as the host population growth would be rapidly diminished. Alternatively, if EhV-86-like genotypes were to be hypothetically the "winners" of these competitive interactions, then this would have resulted in slower infection kinetics which would have allowed the host population to reach higher densities, resulting in a greater total amount of carbon and nutrient re-circulation, over a longer time scale. Ultimately, in a changing marine environment it is important to understand both the phenotypic and genotypic diversity changes that occur within a microbial community and how these changes affect globally important ecological and biogeochemical processes.

The evolutionary significance of intragenus virus competition is the fuelling of the co-evolutionary arms race between the host and its virus. During the described competition scenario, if the two strains were the only ones present in a given environmental niche, then an increase in the fitness of EhV-207 would have resulted in the decrease in fitness of EhV-86 to the point of its extinction or near extinction. Viruses possessing these phenotypes, will infect the most active coccolithophore species and/or strains in consistence with the "killing the winner" hypothesis (Thingstad and Lignell, 1997, Winter et al. 2010), essentially

transforming the host “winners” to “losers” with time. Then, the new host “winners” will most likely be a sub-population that is resistant to EhV-207-like strains but possibly more sensitive to EhV-86-like strains (or other similarly low activity genotypes that have optimal infection strategies for these new host “winners”). This fits within the “virus-host stable co-existence” theory in which was hypothesised the phenotypic plasticity of the algal hosts and their ability to recover post-virus infection, is what makes the co-existence of these hosts and their viruses possible, both on short and also on evolutionary time scales (Thyrhaug et al. 2003).

The emergence of novel viruses with niche-specific characteristics for infection, are to a large extent, a result of these competitive interactions. For instance, in plants, the occurrence of more than one RNA virus and their environmental association with their host is common (Roossinck, 2005). If these viruses are similar to one another then they will be in direct competition, whilst if they are not similar then they will not be. Indeed it was shown that plant RNA virus evolution occurs due to “survival of the fittest” scenario, during which closely related viruses increased the positive selection of some of these viruses over others (Roossinck and Palukaitis, 1995). Thus, the competitive interactions between the closely related coccolithoviruses EhV-86 and EhV-207 may not only drive the fitness and evolution of their hosts, but also their own.

The competitive interactions displayed here by coccolithoviruses raise exciting questions with regards to the ability of these different strains to evolve strategies for the utilisation of new resources; i.e. the infection of a new host. Recently it was shown that resource competition between bacteriophages (i.e. competition over host availability for infection and replication) promoted the evolution of novel bacteriophage phenotypes with the ability to

562 utilise new hosts, suggesting that this sort of competition was essential for driving the
563 evolution of host range expansion (Bono et al., 2013). Although coccolithoviruses are
564 fundamentally different from bacteriophages with regards to their rate of mutation (much
565 slower), a similar resource competition over a larger time scale may explain the large range
566 of susceptible infectious hosts to some coccolithovirus strains (personal observations).
567
568 Furthermore, resource expansion depends most likely also on whether a virus is an r or a K
569 strategist, and the type of trade-offs adapted by viruses and their hosts; a concept that has
570 been applied recently to viruses from the classical life history theory (De Paepe and Taddei,
571 2006, Winter et al, 2010,) . The question of whether a particular virus strain is an r strategist,
572 whereby able to quickly utilize its resource in order to produce abundant virus progenies
573 (usually characterised by a lower percentage of potent virus particles and therefore poor
574 competitors); or a K strategist, whereby the emphasis is on fewer but highly potent,
575 competitive virus progenies, remains to be seen. Based on the classical description of K and r
576 selection theory one would have expected that EhV-86 would have been a better competitor
577 than EhV-207 as it is characterised by slower multiplication rates. However it appears that
578 the latter is a stronger competitor that utilises the available resources quicker and produces a
579 larger number of progeny. Hence both viruses studied here, under optimal conditions, employ
580 aspects of both an R and a K specialist. However, additional factors such as the potential
581 trade-off between high multiplication rates and increased virion decay rates (De Paepe and
582 Taddei, 2006), should also be considered in future studies, particularly under resource-
583 limiting conditions.
584
585 **CONCLUSIONS**

Whether a particular coccolithovirus strain (and all its associated genomic, proteomic, and metabolomic characteristics) will proliferate, is determined by its ability to co-evolve with one or more host genotypes and outcompete other viruses less fit in a particular environment. One can only imagine the complexity of the interactions described here in naturally occurring blooms where at any given time there are many different coccolithophore genotypes (and subsequently phenotypes) and an even larger number of distinct coccolithoviruses, often experiencing annual variable environmental conditions. The dominance of a select few virus genotypes at the end of a bloom or an infection event is a paradox of which the drivers still remain anonymous. However specific characterisation of coccolithovirus genotypes and phenotypic interrogation of their infection dynamics, in tandem with the analysis of their phylogenetic history and functional biodiversity, can shed new light on coccolithovirus evolution and ultimately their role in microbial oceanography.

ACKNOWLEDGMENTS

This work was funded by the NERC Oceans 2025 program, Plymouth Marine Laboratory's Research Program, and a NERC PhD grant awarded to JIN, co-supervised by the Plymouth Marine Laboratory and the University of Nottingham in the UK. We would like to acknowledge Dr. Simon Thomas for providing initial assistance during the qPCR part of the experiments, and also Paul Rooks and Mark Jones for always making sure that the work was conducted in a suitable, tidy and organized environment.

REFERENCES

Allen, M.J., Schroeder, D.C., Donkin, A., Crawfurd, K.J., and Wilson, W.H. (2006) Genome comparison of two Coccolithoviruses. *Virol. J.* **3**: 15.

Bidle, K.D., Haramaty, L., Barcelos E Ramos, J., and Falkowski, P. (2007) Viral activation and recruitment of metacaspases in the unicellular coccolithophore, Emiliania huxleyi. *Proc. Natl. Acad. Sci. U. S. A.* **104**: 6049–54.

613 Bidle, K.D. and Vardi, A. (2011) A chemical arms race at sea mediates algal host-virus
614 interactions. *Curr. Opin. Microbiol.* **14**: 449–57.

615 Bidle, K.D. and Kwityn, C.J. (2012) Assessing the role of caspase activity and metacaspase
616 expression on viral susceptibility of the coccolithophore, Emiliania huxleyi. J. Phycol. **48**:
617 1079–1089.

618 Bono, L.M., Gensel, C.L., Pfennig, D.W., and Burch, C.L. (2013) Competition and the
619 origins of novelty: experimental evolution of niche-width expansion in a virus. *Biol. Lett.* **9**:
620 20120616.

621 Bratbak, G., Levasseur, M., Michaud, S., Cantin, G., Fernández, E., Heimdal, B., and Heldal,
622 M. (1995) Viral activity in relation to Emiliania huxleyi blooms:a mechanism of DMSP
623 release? *Mar. Ecol. Prog. Ser.* **128**: 133–142.

624 Brussaard, C.P.D., Marie, D., and Bratbak, G. (2000) Flow cytometric detection of viruses. *J.*
625 *Virol. Methods* **85**: 175–82.

626 Brussaard, C.P.D. (2004) Optimization of Procedures for Counting Viruses by Flow
627 Cytometry Optimization of Procedures for Counting Viruses by Flow Cytometry. *App and*
628 *Envir. Micro.* **70**: 1506-1513.

629 Brussaard, C.P.D. (2004) Viral control of phytoplankton populations – a review. The Journal
630 of Eukaryotic Microbiology. **51**: 125–138.

631 Brussaard, C.P.D., Wilhelm, S.W., Thingstad, F., Weinbauer, M.G., Bratbak, G., Heldal, M.,
632 et al. (2008) Global-scale processes with a nanoscale drive: the role of marine viruses. *ISME*
633 *J.* **2**: 575–8.

634 Coolen, M.J.L. (2011) 7000 years of Emiliania huxleyi viruses in the Black Sea. *Science* **333**:
635 451–2.

636 De Paepe, M. and Taddei, F. (2006) Viruses' life history: towards a mechanistic basis of a
637 trade-off between survival and reproduction among phages. *PLoS Biol.* **4**: e193.

638 Fuhrman, J.A. (1999) Marine viruses and their biogeochemical and ecological effects. *Nature*
639 **399**: 541–8.

640 Greiner, T., Frohns, F., Kang, M., Van Etten, J.L., Käsmann, A., Moroni, A., et al. (2009)
641 Chlorella viruses prevent multiple infections by depolarizing the host membrane. *J. Gen.*
642 *Virol.* **90**: 2033–9.

643 Han, G., Gable, K., Yan, L., Allen, M.J., Wilson, W.H., Moitra, P., et al. (2006) Expression
644 of a novel marine viral single-chain serine palmitoyltransferase and construction of yeast and
645 mammalian single-chain chimera. *J. Biol. Chem.* **281**: 39935–42.

646 Highfield, A., Evans, C., Walne, A., Miller, P.I., and Schroeder, D.C. (2014) How many
647 Coccolithovirus genotypes does it take to terminate an Emiliania huxleyi bloom? *Virology* in
648 press.

649 Jacquet, S., Heldal, M., Iglesias-Rodriguez, D., Larsen, a, Wilson, W., and Bratbak, G.
650 (2002) Flow cytometric analysis of an Emiliana huxleyi bloom terminated by viral infection.
651 *Aquat. Microb. Ecol.* **27**: 111–124.

652 Kimmance, S., Allen, M., Pagarete, a, Martínez Martínez, J., and Wilson, W. (2014)
653 Reduction in photosystem II efficiency during a virus-controlled Emiliania huxleyi bloom.
654 *Mar. Ecol. Prog. Ser.* **495**: 65–76.

655 Luria, S.E. and Delbruck, M. (1943) Mutations of bacteria from virus sensitivity to virus
656 resistance. *Genetics* **28**: 491–511.
657
658 Markine-Goriaynoff N., Gillet L., Van Etten J.L., Korres H., Verma N., Vanderplasschen A.
659 (2004) Glycosyltransferases encoded by viruses. *J. Gen. Virol.* **85**:2741–2754.

660 Martínez, J.M., Schroeder, D.C., Larsen, A., Bratbak, G., and Wilson, W.H. (2007)
661 Molecular dynamics of Emiliania huxleyi and cooccurring viruses during two separate
662 mesocosm studies. *Appl. Environ. Microbiol.* **73**: 554–62.

663 Martínez, J.M., Schroeder, D.C., and Wilson, W.H. (2012) Dynamics and genotypic
664 composition of Emiliania huxleyi and their co-occurring viruses during a coccolithophore
665 bloom in the North Sea. *FEMS Microbiol. Ecol.* **81**:315–323.

666 Michaelson, L. V, Dunn, T.M., and Napier, J. a (2010) Viral trans-dominant manipulation of
667 algal sphingolipids. *Trends Plant Sci.* **15**: 651–5.

668 Monier, A., Pagarete, A., de Vargas, C., Allen, M.J., Read, B., Claverie, J., et al. (2009)
669 Horizontal gene transfer of an entire metabolic pathway between a eukaryotic alga and its
670 DNA virus. *Genome Res.* **19**: 1441–9.

671 Nissimov, J.I., Worthy, C. a., Rooks, P., Napier, J. a., Kimmance, S. a., Henn, M.R., et al.
672 (2011a) Draft genome sequence of the coccolithovirus EhV-84. *Stand. Genomic Sci.* **5**: 1–11.

673 Nissimov, J.I., Worthy, C. a, Rooks, P., Napier, J. a, Kimmance, S. a, Henn, M.R., et al.
674 (2011b) Draft genome sequence of the Coccolithovirus Emiliania huxleyi virus 203. *J. Virol.*
675 **85**: 13468–9.

676 Nissimov, J.I., Worthy, C. a, Rooks, P., Napier, J. a, Kimmance, S. a, Henn, M.R., et al.
677 (2012a) Draft Genome Sequence of Four Coccolithoviruses: Emiliania huxleyi Virus EhV-
678 88, EhV-201, EhV-207, and EhV-208. *J. Virol.* **86**: 2896–7.

679 Nissimov, J.I., Worthy, C. a, Rooks, P., Napier, J. a, Kimmance, S. a, Henn, M.R., et al.
680 (2012b) Draft Genome Sequence of the Coccolithovirus Emiliania huxleyi Virus 202. *J.*
681 *Virol.* **86**: 2380–1.

682 Nissimov, J.I., Jones, M., Napier, J. a, Munn, C.B., Kimmance, S. a, and Allen, M.J. (2013)
683 Functional inferences of environmental coccolithovirus biodiversity. *Virol. Sin.* **28**: 291–302.

684 Nissimov, J.I. (2013) Ecological and functional biodiversity in a marine algal-virus system :
685 genotypes, phenotypes and their ecological significance. PhD thesis.

686 Nissimov, J.I., Napier, J. a, Kimmance, S. a, and Allen, M.J. (2014) Permanent draft genomes
687 of four new coccolithoviruses: EhV-18, EhV-145, EhV-156 and EhV-164. *Mar. Genomics*
688 **15**: 7–8.

689 Pagarete, A., Allen, M.J., Wilson, W.H., Kimmance, S. a, and de Vargas, C. (2009) Host-
690 virus shift of the sphingolipid pathway along an Emiliania huxleyi bloom: survival of the
691 fattest. *Environ. Microbiol.* **11**: 2840–8.

692 Pagarete, a, Lanzén, a, Puntervoll, P., Sandaa, R. a, Larsen, a, Larsen, J.B., et al. (2013)
693 Genomic sequence and analysis of EhV-99B1, a new coccolithovirus from the Norwegian
694 fjords. *Intervirology* **56**: 60–6.

695 Pagarete, A., Kusonmano, K., Petersen, K., Kimmance, S. a, Martínez Martínez, J., Wilson,
696 W.H., et al. (2014) Dip in the gene pool: Metagenomic survey of natural coccolithovirus
697 communities. *Virology* In press, 1–9.

698 Parada, P., Herndl, G.J., O, M.G.W., and Burg, N.-A.B. Den (2006) Viral burst size of
699 heterotrophic prokaryotes in aquatic systems. *J. Mar. Biol. Assoc. UK*. **86**: 613–621.

700 Roossinck, M.J. and Palukaitis, P. (1995) Genetic analysis of helper virus-specific selective
701 amplification of cucumber mosaic virus satellite RNAs. *J. Mol. Evol.* **40**: 25–29.

702 Rowe, J.M., Fabre, M.-F., Gobena, D., Wilson, W.H., and Wilhelm, S.W. (2011) Application
703 of the major capsid protein as a marker of the phylogenetic diversity of Emiliania huxleyi
704 viruses. *FEMS Microbiol. Ecol.* **76**: 373–80.

705 Schroeder, D.C., Oke, J., Malin, G., and Wilson, W.H. (2002) Coccolithovirus
706 (Phycodnaviridae): characterisation of a new large dsDNA algal virus that infects Emiliana
707 huxleyi. *Arch. Virol.* **147**: 1685–98.

708 Schroeder, D.C., Oke, J., Hall, M., Malin, G., and Wilson, W.H.W.H. (2003) Virus
709 succession observed during an Emiliania huxleyi bloom. *Appl. Environ. Microbiol.* **69**: 2484.

710 Sorensen, G., Baker, A.C., Hall, M.J., Munn, C.B., and Schroeder, D.C. (2009) Novel virus
711 dynamics in an Emiliania huxleyi bloom. *J. Plankton Res.* **31**: 787–791.

712 Thingstad, T. and Lignell, R. (1997) Theoretical models for the control of bacterial growth
713 rate, abundance, diversity and carbon demand. *Aquat. Microb. Ecol.* **13**: 19–27.

714 Thyrhaug, R., Larsen, a, Thingstad, T., and Bratbak, G. (2003) Stable coexistence in marine
715 algal host-virus systems. *Mar. Ecol. Prog. Ser.* **254**: 27–35.

716 Vardi, A., Van Mooy, B.A.S.B. a S., Fredricks, H.F.H.F., Popendorf, K.J.K.J., Ossolinski,
717 J.E.J.E., Haramaty, L., and Bidle, K.D.K.D. (2009) Viral glycosphingolipids induce lytic
718 infection and cell death in marine phytoplankton. *Science* **326**: 861–5.

719 Vardi, A., Haramaty, L., Mooy, B.A.S. Van, Fredricks, H.F., Kimmance, S.A., and Larsen,
720 A. (2012) Host – virus dynamics and subcellular controls of cell fate in a natural
721 coccolithophore population. **109**: 19327–19332.

722 Wilson, W. and Mann, N. (1997) Lysogenic and lytic viral production in marine microbial
723 communities. *Aquat. Microb. Ecol.* **13**: 95–100.

724 Wilhelm, S.W. and Suttle, C.A. (1999) Viruses and Nutrient Cycles in the Sea. *BioScience*
725 **49**: 781-788.

726 Wilson, W.H., Tarran, G.A., Schroeder, D., Cox, M., Oke, J., and Malin, G. (2002) Isolation
727 of viruses responsible for the demise of an Emiliania huxleyi bloom in the English Channel.
728 *J. Mar. Biol. Assoc. UK* **82**: 369–377.

729 Winter, C., Bouvier, T., Weinbauer, M.G., and Thingstad, T.F. (2010) Trade-offs between
730 competition and defense specialists among unicellular planktonic organisms: the "killing the
731 winner" hypothesis revisited. *Microbiol. Mol. Biol. Rev.* **74**: 42–57.

732 Zhang, Y., Xiang, Y., Van Etten, J.L., and Rossmann, M.G. (2007) Structure and function of
733 a chlorella virus-encoded glycosyltransferase. *Structure* **15**: 1031–9.

734

735

736

737

738

739

740

741

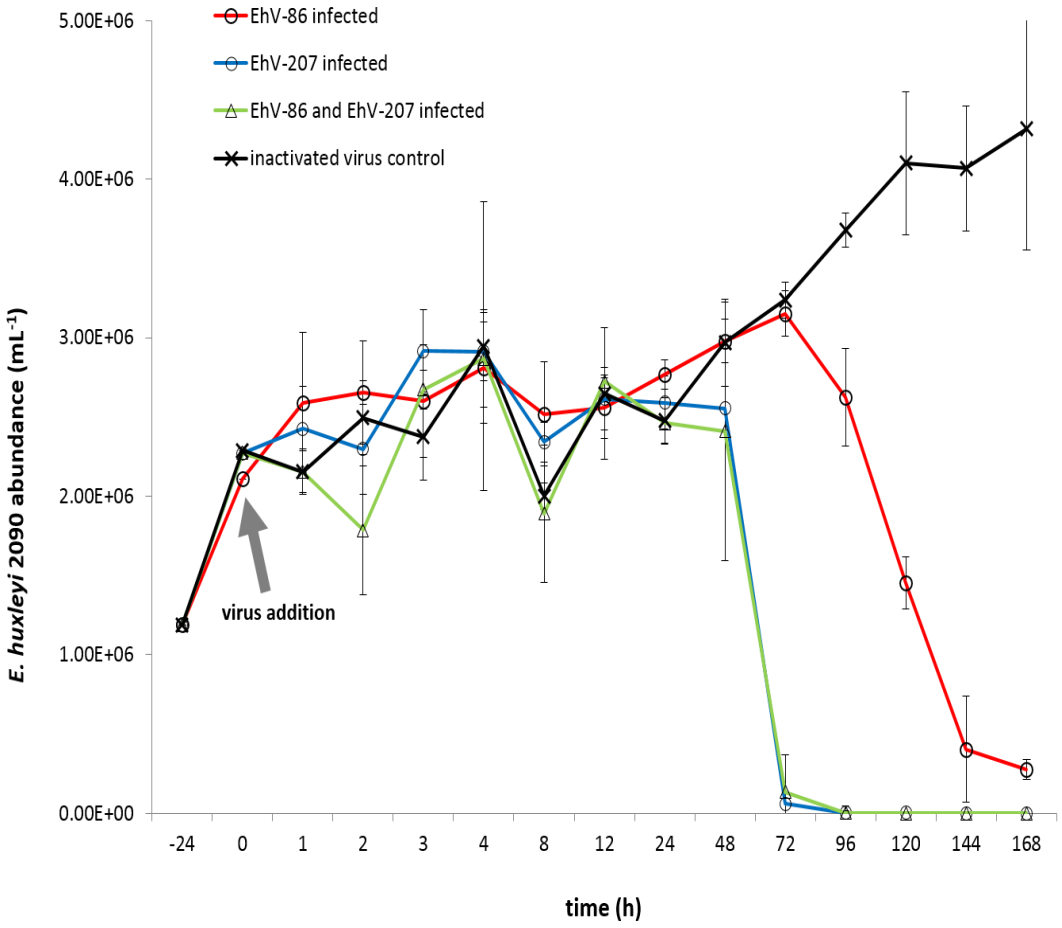

742

743 **Fig. 1.** *Emiliania huxleyi* CCMP 2090 average cells mL^{-1} (triplicates ±SD) following
744 infection by EhV-86 (red line) EhV-207 (blue line), and combined EhV-86 and EhV-207
745 (green line). Control cultures containing inactivated viruses are shown by theblack line. The
746 first measurements of the host cultures taken one day before the addition of the virus stocks
747 (i.e. t -24 h).
748

749

750
751

752

753

754

755

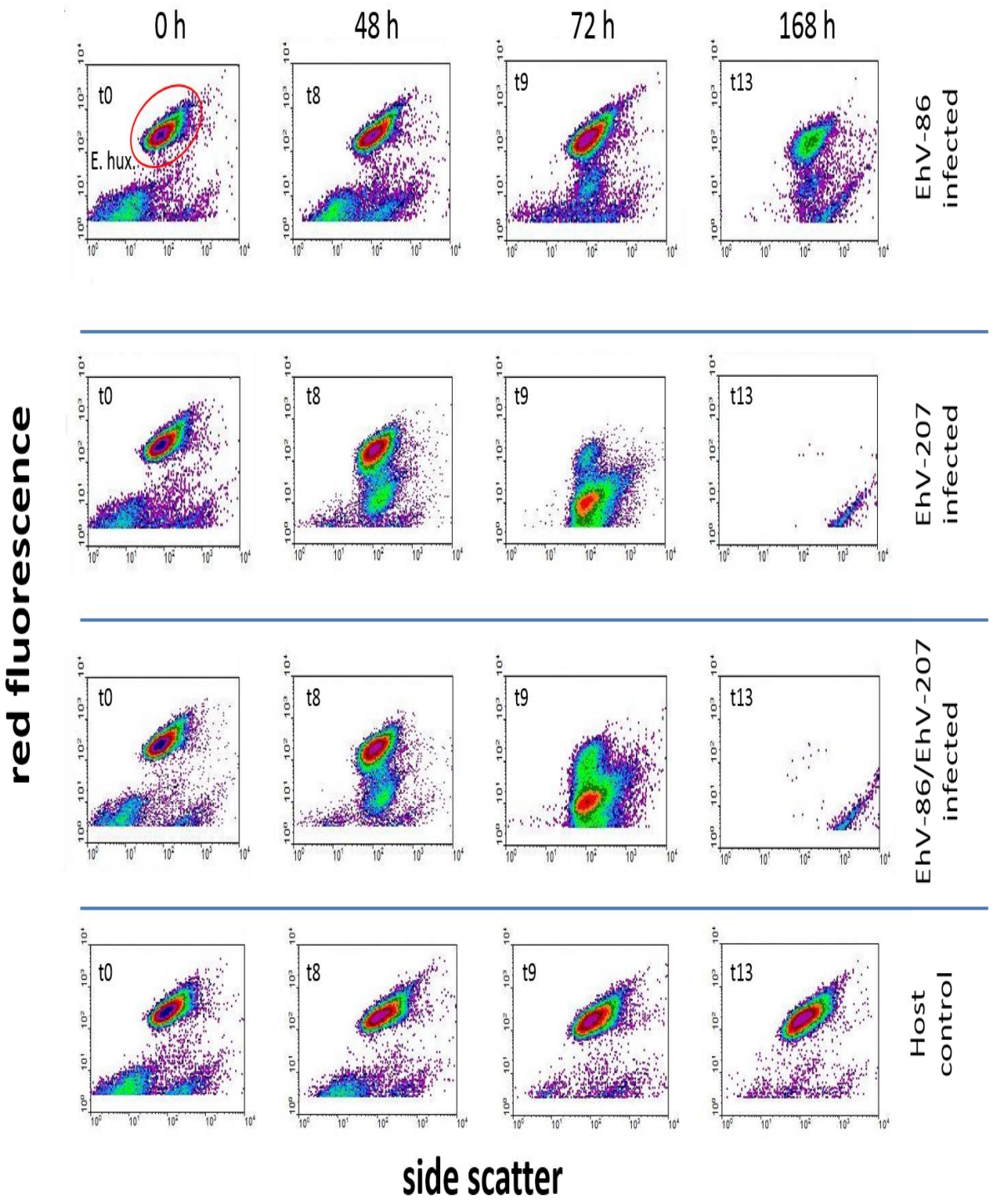

Fig. 2. Flow cytometry plots of red (chlorophyll) fluorescence versus side scatter at 0 h and 168 h during the time course experiment for infected (EhV-86, EhV-207 or combined EhV-86&EhV-207 co-infected) and control *Emiliania huxleyi* cultures.

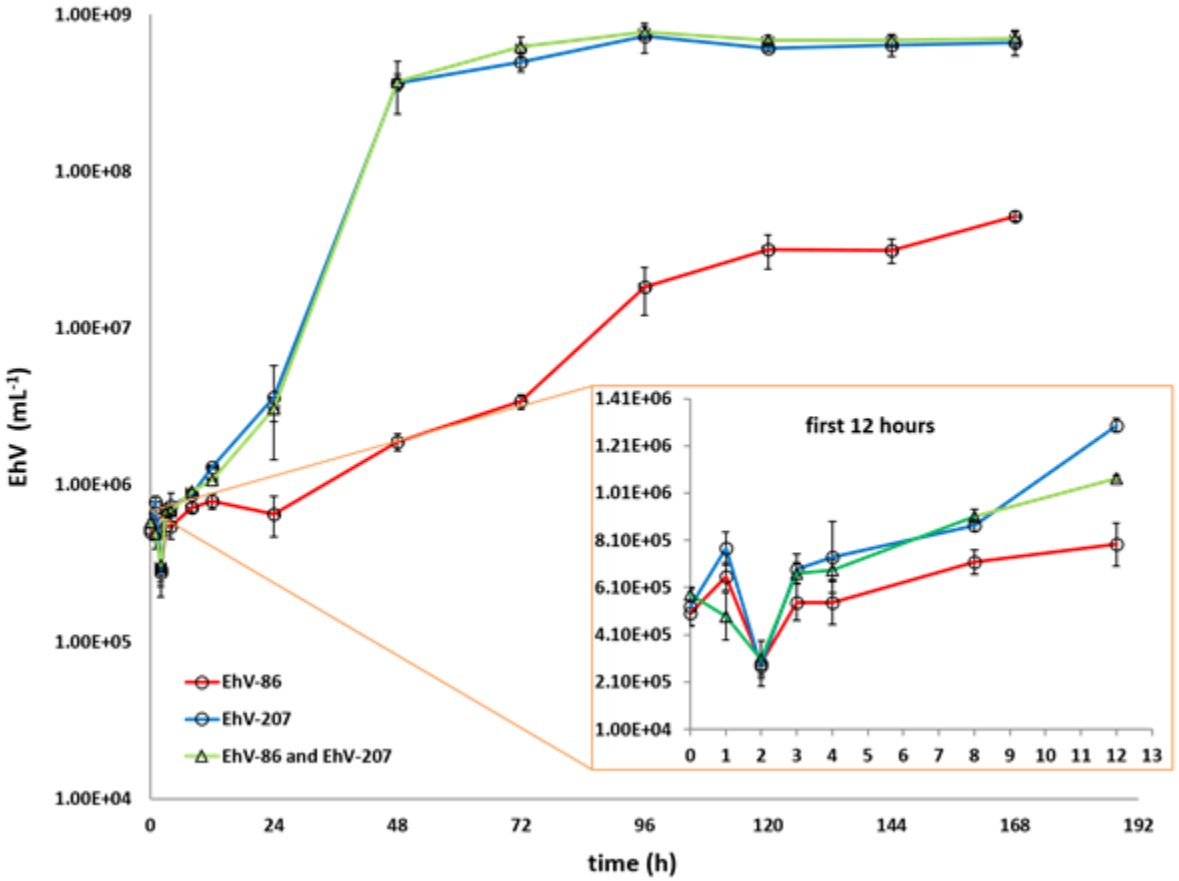

761

762

763 **Fig. 3.** Average density $mL^{-1}$of EhV-86 (red line), EhV-207 (blue line), and combined EhV-
764 86&EhV-207 (green line) during the time-course experiment. Data points represent triplicate
765 measurements (±SD). The abundance of free EhVs was enumerated using AFC (green
766 fluorescence *vs* side scatter).

767

768

769

770

771

772

773

774

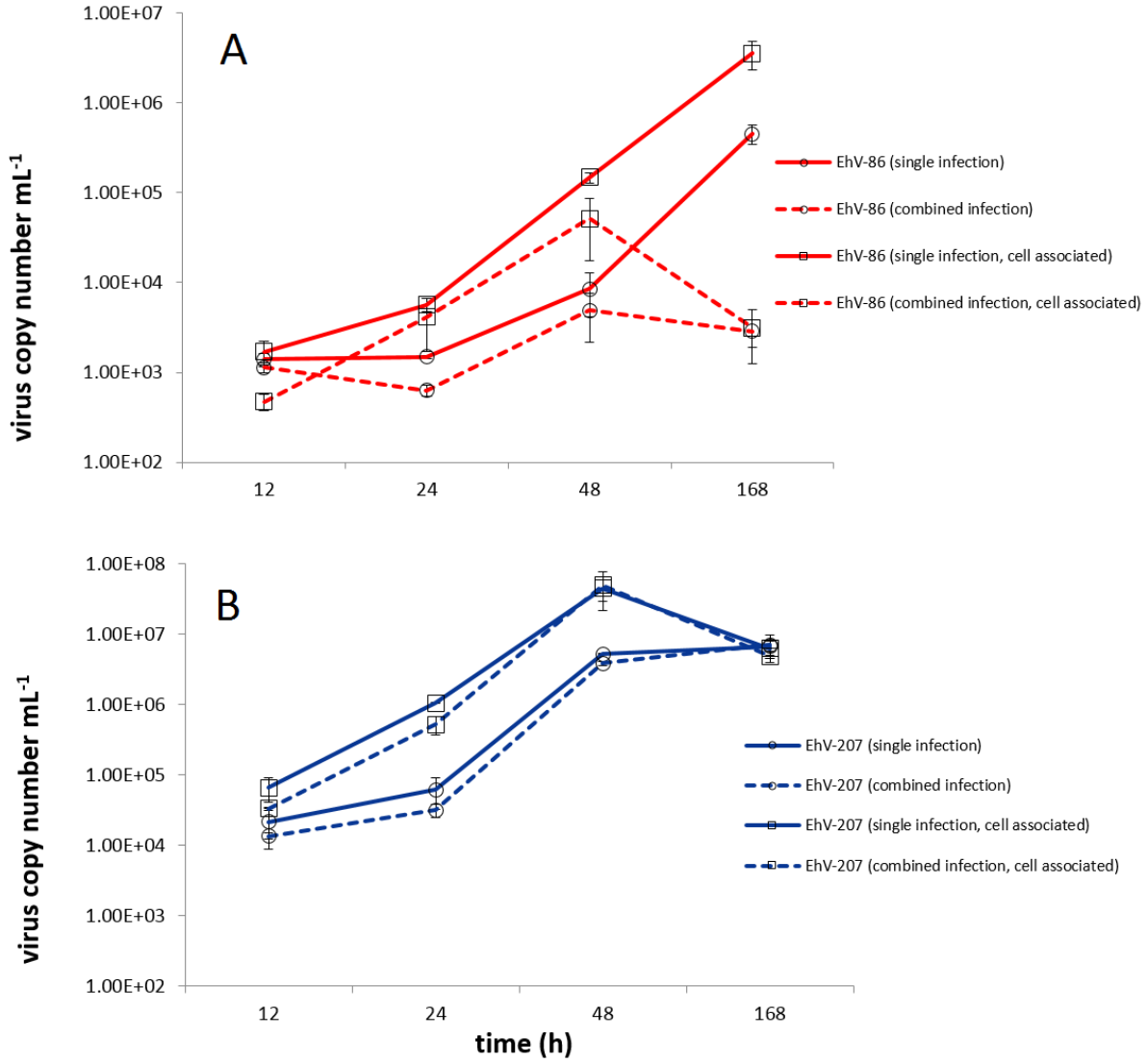

Fig. 4. EhV-86 (A) and EhV-207 (B) virus copy number averages (triplicates ± SD) from *Emiliania huxleyi* cultures infected with either EhV-86 (single infection), EhV-207 (single infection) or combined EhV-86&EhV-207 (combined infection), 12 h, 24 h, 48 h and 168 h post infection; performed with qPCR strain specific primers for the discrimination of one coccolithovirus strain from the other.

Table S1. Virus treatments A-G and their initial volume* at the beginning of the experiment (t0). Each treatment was performed in triplicate (i.e. a total of 21 flasks; 12 containing *E. huxleyi* CCMP 2090 at a cellular density of 1.5×10^6 mL^{-1}). + indicates the presence of EhV-86, EhV-207, or host in a given flask, – indicates inactivated virus.

Flask n°	**Volume of f/2 media (mL)***	**EhV-86**	**EhV-207**	***E.huxleyi* host**	**Experimental treatment**
1	100	+		+	
2	100	+		+	A
3	100	+		+	
4	100		+	+	
5	100		+	+	B
6	100		+	+	
7	100	+	+	+	
8	100	+	+	+	C
9	100	+	+	+	
10	100	+			
11	100	+			D
12	100	+			
13	100		+		
14	100		+		E
15	100		+		
16	100	+	+		
17	100	+	+		F
18	100	+	+		
19	100	-	-	+	
20	100	-	-	+	G
21	100	-	-	+	

Table S2. Free, unattached, average (triplicate) EhV abundance and virus copy number (VCN) per mL, detected by analytical flow cytometry (AFC) and quantitative polymerase chain reaction (qPCR) respectively, 12 h and 168 h post-addition of viruses; either EhV-86 or EhV-207.

Analysis type	**AFC**	**qPCR**	**AFC**	**qPCR**
time (h)	**EhV-86 (solo free)**	**EhV-86 (solo free)**	**EhV-207 (solo free)**	**EhV-207 (solo free)**
12	**7.92×10^5**	**1.40×10^3**	**1.30×10^6**	**2.14×10^4**
168	**5.19×10^7**	**4.51×10^5**	**6.58×10^8**	**6.71×10^6**

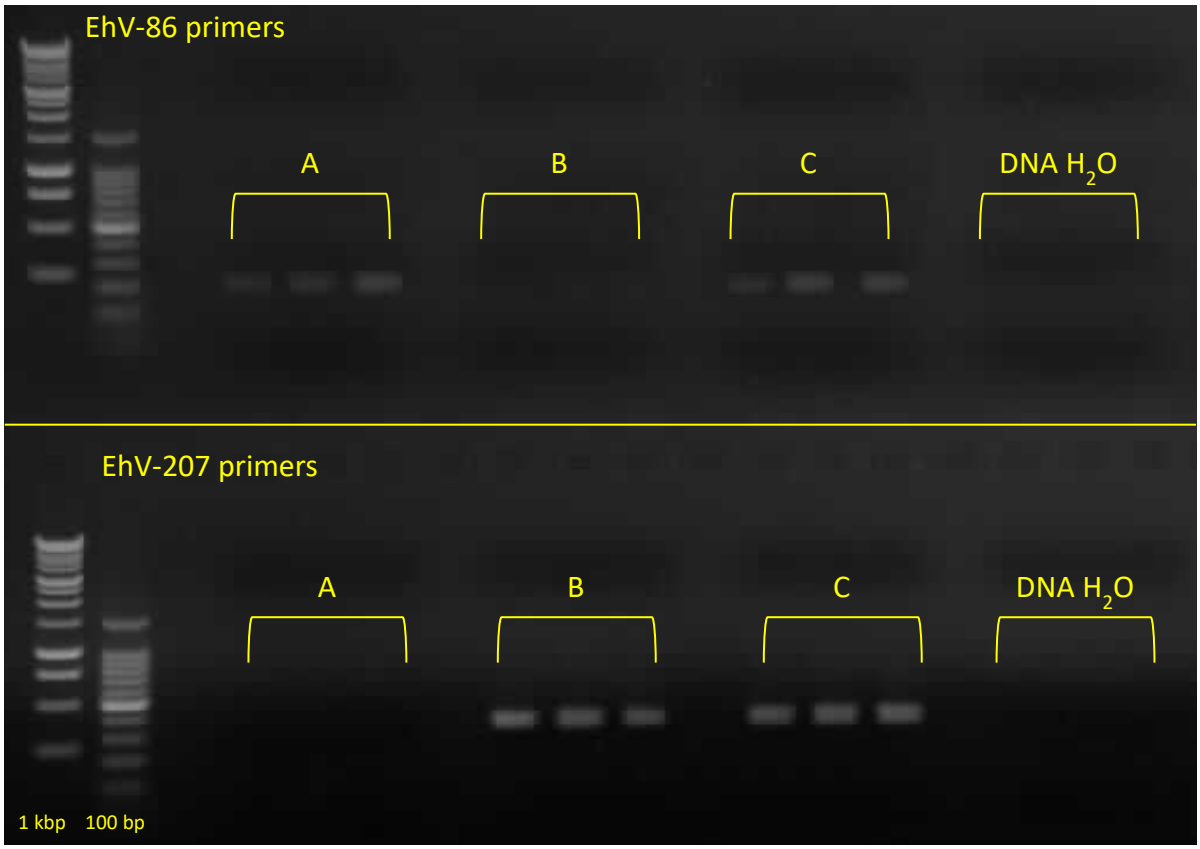

Fig. S1. Gel electrophoresis of PCR products conducted with primers specific to EhV-86 and EhV-207. The products are amplified regions from lysates taken from three different culture conditions: EhV-86 infected host (A), EhV-207 infected host (B), and host infected simultaneously by both EhV-86 and EhV-207 (C). In the last two lanes to the right (top and bottom) are the control DNA free water samples.

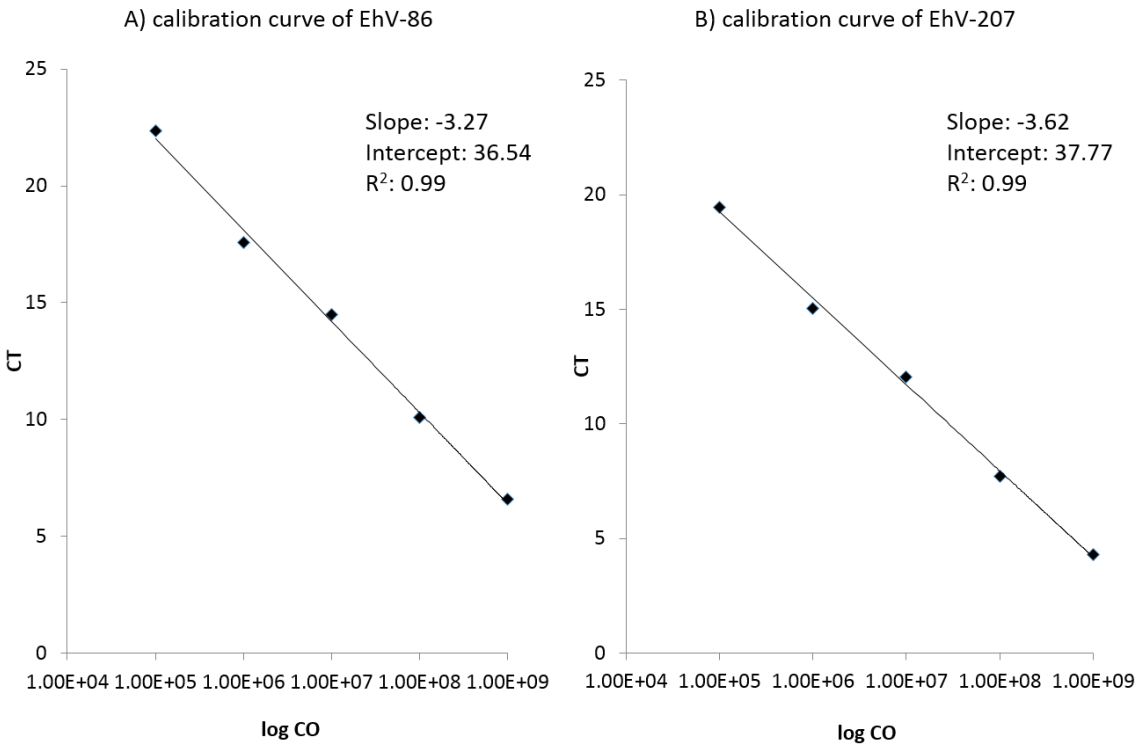

850

851 **Fig. S2.** Calibration curve for the qPCR amplification of known amounts of purified DNA of
852 EhV-86 (ehv290) and EhV-207 (EQVG00465). CT= cycle number, (log CO= known
853 concentrations of purified EhV-86 (A) and EhV-207 (B) DNA products.

854
855

856

857